Potential Energy Surfaces of Vinylogous Wolff Rearrangement: NBO Analysis and Molecular Dynamic Simulation

Hossein Taherpour Nahzomi*[a] and Faten Divsar[b]

The potential energy surfaces of the Vinylogous Wolff Rearrangement, an alternative process for the Wolff Rearrangement that takes place β,γ-unsaturated diazoketones have been fully explored employing M062X model chemistry and in a complementary task by means of the CASSCF method. The NBO analysis has been invoked to reveal the alternations of orbital occupancies and their stabilization energies through some of the critical structures located on the pathways. The calculations establish a two steps process for each pathway involving a second higher energy transition state that seems likely to be the rate determining step in agreement with experimental results. Energy analysis indicates more feasibility of the pathway including diradical intermediate. The most striking feature of the study concerns the finding out a transition state providing a channel in between two pathways through interconversion of the two keys bicyclo[2.1.0]pentanone and diradical intermediates.

The well-known Vinylogous Wolff Rearrangement (VWR) has resulted in a particular interest from a mechanistic point of view, in the case of β,γ-unsaturated diazoketone, which was found to behave in a different manner than in the traditional Wolff Rearrangement (WR) under the same reaction condition. This route provides a convenient method for the synthesis of rearranged γ,ϰ-unsaturated-acid derivatives, while the Wolff Rearrangement leads to homologation of carboxylic acids.

Mechanistically, the involvement of a highly strained bicyclo [2.1.0]pentanone intermediate has been suggested, which in turn originated from an intramolecular carbenoid addition into the double bond in a previous reaction step. Subsequently, a fragmentation through a retro-[2 + 2] cycloaddition leads to the β,γ-unsaturated ketene intermediate susceptible to be trapped by a nucleophile such as CH_3OH to provide the rearranged γ, ϰ-unsaturated ester. The postulation of the presence of a bicyclo [2.1.0]pentanone intermediate and subsequently fragmentation to the corresponding ketene have been emerged from the early works of Stork,[1] Gutsh,[2] Wilds,[3] Masamune[4] and Bond.[5]

There are some examples revealing the extension of the scope of the VWR as an efficient synthetic route,[6] such as the preparation of angularly functionalized polycyclic systems,[7] synthesis of substituted malonates,[8] affording mono-, bi- and tricyclic piperidone compounds,[9] and preparation of α-Diazo Sulfoxides[10] besides of α-diazo carbonyl compounds.[11] The conversion of ketenes into carboxylic acids, esters, or amides is also an important step in synthetic applications of the Wolff rearrangement.[6]

A variety of efficient catalysts have been used to promote the VWR, such as copper (II) sulfate, copper (II) bis (acetylacetonato), copper (II) bis (trifluoromethylsulphonate), silver (I) benzoate and Rh2(OAc)4, titanium tetrachloride.[12] Amos B. Smith was the first who has studied the VWR extensively and based on a stepwise manner proposed the following equation to justify the conversion of the diazo ketone compound into the corresponding ketene through providing the supportive data, (Scheme 1).[13] Also the possibility of the interconversion between bicyclo[2.1.0] pentanone and a zwitterionic/diradical intermediate has been considered.

Surprisingly, despite the attractive features of this skeletal rearrangement there is not any computational study about it. At the present study the Potential Energy Surface (PES) of the whole reaction pathway will be explored aiming to determine the structures of transition states and intermediates and hence the corresponding energy barriers. Besides that, the possibility

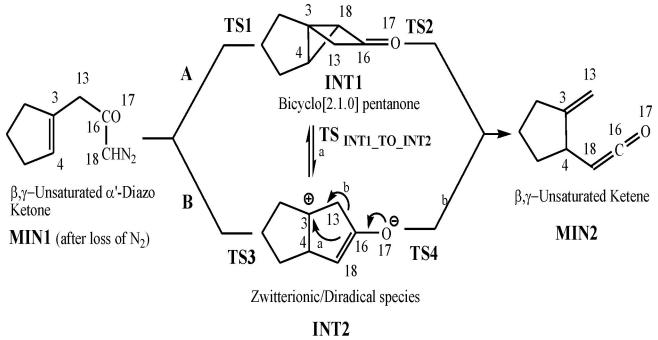

Scheme 1. The Mechanism of Conversion of the Diazo Ketone Compound into the Corresponding Ketene.

[a] *Dr. H. T. Nahzomi*
Department of Chemistry
Payame Noor University
PO BOX 19395-3697, Tehran (Iran)
E-mail: h_taherpour@pnu.ac.ir
[b] *Dr. F. Divsar*
Department of Chemistry
Payame Noor University
PO BOX 19395-3697, Tehran (Iran)

Supporting information for this article is available on the WWW under https://doi.org/10.1002/open.202100049

of bicyclo into dipolar/diradical species interconversion are considered. Finally, these energy barriers along with the NBO analysis and molecular dynamic simulations would be invoked to account for the dominant reaction pathway.

All Quantum mechanical calculations carried out employing the Gaussian 09 program.[14] The located geometries of all structures obtained by DFT and the M062X exchange-correlation functional as implemented in Gaussian 09[15] in combination with the 6–31 + + G(2d,p) basis sets for Carbon, Hydrogen, and Oxygen atoms. The odd electron density (OED) calculation performed employing Multiwfn program.[16] Molecular dynamic simulations of some of the located transition states carried out using deMon software.[17] The resulted simulation can be viewed with interface to visualization software Molden.

According to the calculations, two reaction pathways have been explored, each of which may be considered as a two steps process that share in common the initial structure labeled as MIN1, the carbene that is produced by departure of N2 group from the first diazoketone molecule as starting compound by treatment with the employed catalyst as well as the last structure labeled MIN2, the corresponding ketene. The located structures are represented in (Figure 1) and their energies, relative energies and energy barriers are collected in (Table 1), while (Figure 2) displays the reaction profiles of the two competitive pathways (A and B).

Pathway A initiates by addition of C18 into C3=C4 double bond through TS1 which lies 0.05 Kcal mol^{-1} above the MIN1. This very low energy barrier is remarkable and could be explained by considering that MIN1 is in turn a high energy molecule. Imaginary frequency in TS1 represents the movement of C18 toward the C3=C4 double bond. From the NBO analysis results involved in Table 2 it appears that C16–C18 bond has pi character in MIN1 that extensively diminishes in TS1, the delocalizations such as $\pi_{C16-O17} \rightarrow \pi^*_{C16-C18}$ and $\pi_{C16-C18} \rightarrow \pi^*_{C16-O17}$ provide considerable stabilizations in MIN1. Transformation of MIN1 into TS1 leads to some structural deformations, for instance the C16–C18 bond length is elongated by the amount of 0.04 A°, the bond angle O17–C16–C18 is increased by the value of 12.6 degree and O17–C16–C18–H dihedral angle is reduced by the extent of 4.4 degree. This evolution destructs the pi character of C16–C18 and consequently two new orbitals involving bonding $n_{C18(1)}$ and antibonding $n^*_{C18(2)}$ located at C18 center respectively with occupancies of 1.77181 and 0.25350 are appeared. Where does the occupancy of $n^*_{C18(2)}$ come from? Again from the data of (Table 2) it would be clear that the delocalizations such as $\pi_{C16-O17} \rightarrow n^*_{C18(2)}$ and $n_{O17(2)} \rightarrow n^*_{C18(2)}$ have the most contributions and the $\pi_{C3-C4} \rightarrow n^*_{C18(2)}$ the least participation. Such a subtle structural deformations and slight interaction between π_{C3-C4} and $n^*_{C18(2)}$ and very low energy barrier altogether are pointing to the fact that TS1 seems likely to be an early transition state.

By evaluating the molecular orbitals of TS1 it would be understood that the molecular orbital number 32, i.e., HOMO-1 takes part in the interaction between C3=C4 and C18, (Figure 3-a).

Following the process bicyclo[2.1.0] pentanone is produced as an intermediate, INT1. Regarding this structure NBO analysis

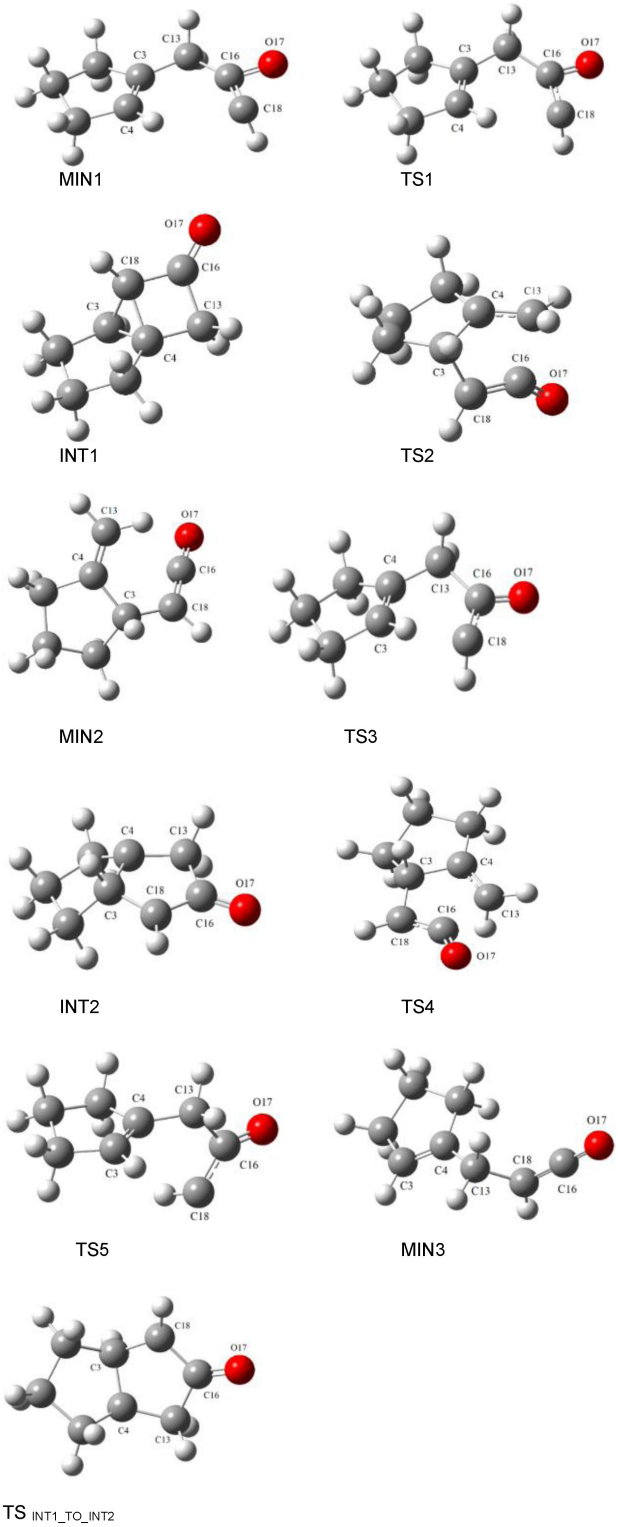

Figure 1. Optimized geometries obtained at M062X/6-31 + + G(2d,p) level of theory.

reveals the improvement of pi character of $\pi_{C16-O17}$ as well as occupancies of $n_{O17(1)}$ and $n_{O17(2)}$. Proceeding the reaction INT1 undergoes two concurrent bond dissociation through TS2 which is 20.37 Kcal mol^{-1} higher in energy than INT1 and

Table 1. Calculated Energies Obtained at the M062X/6-31++G[2d, p] and CASSCF(6,6)/6-31++G[2d, p] Level of Theory.

Structure	Energy[a] [hartree]	Rel. Energy [Kcal mol^{-1}]	E_a [Kcal mol^{-1}]
M062X			
MIN1	−385.633238	0.00	0.05
TS1	−385.633156	0.05	
INT1	−385.735691	−64.29	20.37
TS2	−385.703225	−43.92	
MIN2	−385.743034	−68.90	
MIN1	−385.633238	0.00	0.24
TS3	−385.632855	0.24	
INT2	−385.689635	−35.38	14.24
TS4	−385.666930	−21.14	
MIN2	−385.743034	−68.90	
MIN1	−385.633238	0.00	1.89
TS5	−385.630225	1.89	
MIN3	−385.745074	−70.18	
CASSCF(6,6)			
INT1_CAS	−383.500789	0.00	8.09
$TS_{INT1\_TO\_INT2}$	−383.487895	8.09	

[a] E0elec + ZPVE.

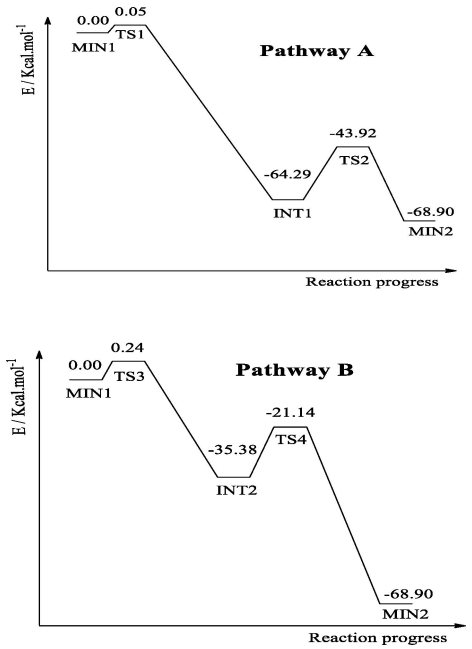

Figure 2. Two competitive reaction profiles of Vinylogous Wolff Rearrangement.

involves both C4–C18 and C13–C16 bonds cleavage congruently and eventually gives the final product as a ketene. Some noteworthy points about pathway B are as follow; TS3 is the transition state that appropriately connect MIN1 to INT2 and represents the movement of C3 and C18 atoms toward each other, the corresponding activation energy estimated to be 0.24 Kcal mol^{-1}, slightly higher than that of TS1. The C3–C18 distance in TS1 and TS3 are 3.00 and 2.43 A°, respectively. Hence in TS3, C3 and C18 atoms become closer to each other and as a result the interaction and delocalization such as $\pi_{C3-C4} \rightarrow n^*_{C18(2)}$ would be greater. Comparing some structural parameters in between MIN1 and TS3 reveals that the C16–C18

Table 2. NBO Occupancies and Stabilization Energies[Kcal mol^{-1}] Characterizing MIN1, TS1, INT1, TS3 and INT2 Obtained at the M062X/6-31++G[2d, p] Level of Theory.

Orbital	Occupancy	Delocalization	Stabilization Energy [E_2]
MIN1			
π_{C3-C4}	1.94404	$\pi_{C16-O17} \rightarrow \pi^*_{C16-C18}$	74.70
$\pi_{C16-O17}$	1.85022	$\pi_{C16-C18} \rightarrow \pi^*_{C16-O17}$	135.11
$\pi_{C16-C18}$	1.70872	$\pi_{C16-C18} \rightarrow \pi^*_{C16-C18}$	27.69
$n_{O17(1)}$	1.98709	$n_{O17(1)} \rightarrow \pi^*_{C16-C18}$	0.92
TS1			
π_{C3-C4}	1.94217	$\pi_{C16-O17} \rightarrow n^*_{C18(2)}$	17.52
$\pi_{C16-O17}$	1.95246	$n_{O17(2)} \rightarrow n^*_{C18(2)}$	40.92
$n_{O17(1)}$	1.98282	$n_{O17(2)} \rightarrow \pi^*_{C16-O17}$	6.63
$n_{O17(2)}$	1.70659	$n_{C18(1)} \rightarrow \pi^*_{C16-O17}$	4.13
$n_{C18(1)}$	1.77181	$n_{C18(2)} \rightarrow \pi^*_{C16-O17}$	3.45
$n^*_{C18(2)}$	0.25350	$\pi_{C3-C4} \rightarrow n^*_{C18(2)}$	0.77
INT1			
$n_{O17(1)}$	1.97548	$n_{O17(2)} \rightarrow \sigma^*_{C13-C16}$	32.63
$n_{O17(2)}$	1.86134	$n_{O17(2)} \rightarrow \sigma^*_{C16-C18}$	28.66
σ_{C4-C18}	1.88190	$\sigma_{C4-C18} \rightarrow \pi^*_{C16-O17}$	4.38
$\pi_{C16-O17}$	1.99001	$\sigma_{C13-H14} \rightarrow \pi^*_{C16-O17}$	4.86
$\sigma^*_{C13-C16}$	0.07679	$\sigma_{C13-H15} \rightarrow \pi^*_{C16-O17}$	3.13
$\sigma^*_{C16-C18}$	0.06964		
$\pi^*_{C16-O17}$	0.10460		
TS3			
$n_{O17(1)}$	1.97793	$\pi_{C3-C4} \rightarrow n^*_{C18(2)}$	7.74
$n_{O17(2)}$	1.82630	$\pi_{C3-C4} \rightarrow \pi^*_{C16-O17}$	0.58
$n_{C18(1)}$	1.79946	$\pi_{C16-O17} \rightarrow n^*_{C18(2)}$	3.55
$n^*_{C18(2)}$	0.21732	$n_{O17(2)} \rightarrow n^*_{C18(2)}$	8.64
π_{C3-C4}	1.91019	$n_{O17(2)} \rightarrow \pi^*_{C16-C18}$	23.29
		$n_{C18(1)} \rightarrow \pi^*_{C16-O17}$	4.53
		$n_{C18(2)} \rightarrow \pi^*_{C16-O17}$	3.31
INT2			
$\pi_{C16-C18}$	1.64081	$n_{O17(1)} \rightarrow \sigma^*_{C16-C18}$	3.18
$\pi^*_{C16-C18}$	0.37544	$n_{O17(2)} \rightarrow \pi^*_{C16-C18}$	5.64
$n_{O17(1)}$	1.97647	$\pi_{C16-C18} \rightarrow \pi^*_{C16-C18}$	2.15
$n_{O17(2)}$	1.83998		

bond length is elongated by the amount of 0.09 A°, the bond angle O17–C16–C18 is increased by the value of 29.4 degree and O17–C16–C18–H dihedral angle is reduced by the extent of 8.4 degree. As expected, more structure deformation requirements to reach TS3 means the later transition state relative to TS1. Again during this step pi character of C16–C18 is greatly diminished and instead the occupancies at $n_{C18(1)}$ and $n^*_{C18(2)}$ are grown up, obviously delocalizations such as $\pi_{C3-C4} \rightarrow n^*_{C18(2)}$, $\pi_{C16-O17} \rightarrow n^*_{C18(2)}$ and $n_{O17(2)} \rightarrow n^*_{C18(2)}$ counterpart in providing the significant occupancy of $n^*_{C18(2)}$. Following this step chemical bond between C3 and C18 is totally formed which leads to the appearance of INT2 being by the value of 28.91 Kcal mol^{-1} less stable than INT1. To acquire more information about the electron density distribution in INT2, the odd electron density (OED) calculation has been performed employing Multiwfn program. The isosurface map with isovalue of 0.005 is represented in (Figure 3-b) (its character is quite similar with spin density map). It is realized that electron density mostly and nearly in equal amount located at C4 and C18 centers and in less extent at O17 because of the partial resonance present in C18–C16–O17 moiety. This may be an

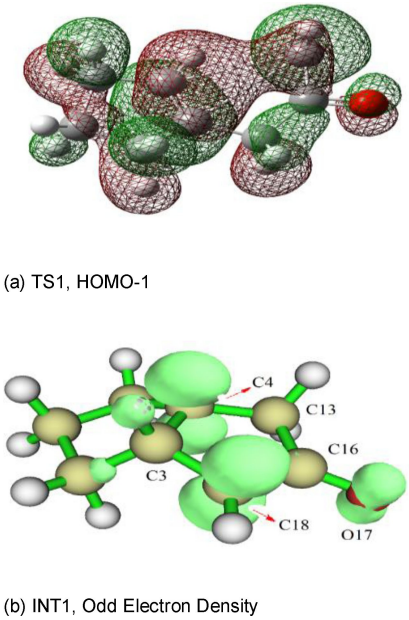

Figure 3. (a), HOMO-1, The most effective orbital participating in ring closure, (b) Odd Electron Density, Odd Electron Density similar with spin density map.

argument to support the postulation of the presence of diradical character of INT2. Finally, this high energy intermediate by overcoming the energy barrier of 14.24 Kcal mol^{-1} through TS4 which involves C13–C16 bond cleavage would yield the corresponding ketene MIN2.

Part of the attempt related to investigate about the possibility of conversion of INT1 into INT2 through three membered ring opening (C18–C3–C4) involving C3–C18 bond cleavage. All the calculations employing M062X and also B3LYP model chemistries resulted in the same TS as like as TS2 ultimately giving rise to MIN2 not INT2. Then, turning to apply Complete Active Space Self Consistent Field model including 6 orbitals and 6 electrons, CASSCF (6,6), the most striking feature of the job continued to be appear. With this regard, TS INT1_TO_INT2, the central and key point of the smith work as well as our calculation obtained. Refining the INT1 by means of CASSCF leads to INT1_CAS, now the required energy to reach TS INT1_TO_INT2 through detachment of C3–C18 bond is calculated to be 8.09 Kcal mol^{-1}. Finding out such a low energy barrier TS opens up a new gate between the present pathways, and the competition in between TS2 and TS INT1_TO_INT2 in favor of the later one that would make a pathway exchange more likely should seriously be considered and as a conse-quence the possibility of the presence of the diradical intermediate, INT2, gains more support.

Investigating the Wolff Rearrangement (WR) in order to compare with VWR is a complementary task aiming to determine the feasibility of such a transformation. Leading on the calculation, TS5 that represents a simultaneous C13–C16 bond breakage as well as C13–C18 bond formation through bending the C13–C16–C18 angle, by the energy barrier of amount 1.89 Kcal mol^{-1} obtained which in turn yields MIN3, the product of the WR through C13 migration as the most stable structure in the Table 1. As the rearrangement proceeds through TS5, C13 and C18 atoms becomes closer and the pi character of the C16=C18 is decreased in TS5 relative to MIN1, but MIN3 as a ketene has shortest C16=C18 bond length amongst these three (1.31 A°). This rearrangement is accompanied by the rotation about C4–C13 single bond. For this reason the C3–C4–C13–C16 dihedral angle in MIN1 and TS5 is 9.42 and 103.83 degree, respectively. The reaction profiles of the Wolff Rearrangement pathway is represented in Figure 4. Comparing the energy barriers to overcoming the TS2, TS4 and TS5, the reason of preferential formation of WR over VWR product in most and ordinary conditions would be realized.

Molecular Dynamic Simulation: Four MD simulations initiated from, TS2, TS4, TS5 and TS INT1_TO_INT2 performed employing deMon program em-ploying the velocity Verlet algorithm, the DZVP-GGA basis and the PBE potential. The simulation run 100 MD steps with a time step of 0.5 fs and write the tra-jectory output at each two iterations. The thermostat is switched on (BATH NOSE) with Temperature set to 600 K. The initial velocities are generated in a random manner (T = 1200 K). The calculation requests a tight numerical tolerance to have a very good quality of energy gradients. They represent conversion of INT1 into MIN2, INT2 into MIN2, MIN1 into MIN3 and INT1 into INT2, respectively. They are included in supplementary information and can be viewed by means of Molden software.

In summary, the potential energy surface of Vinylogous Wolff Rear-rangement has been entirely explored. The results indicate that the first step of each pathway has very low energy barrier and establishes a fast equilibrium between MIN1 and INT1 in one side and between MIN1 and INT2 in the other side. Also the transformation of bicyclo[2.1.0]pentanone intermediate (INT1) into diradical intermediate (INT2) seems likely to be much feasible overcoming a relatively low energy barrier transition state TS INT1_TO_INT2. Following the process through either TS2 or TS4 the corresponding ketene is obtained, while the conver-sion involving diradical intermediate requires lower energy and may be considered as the dominant pathway. Besides that, the calculations show that Wolff Rearrangement needs lower energy to take place comparing to Vinylogous Wolff Rearrangement.

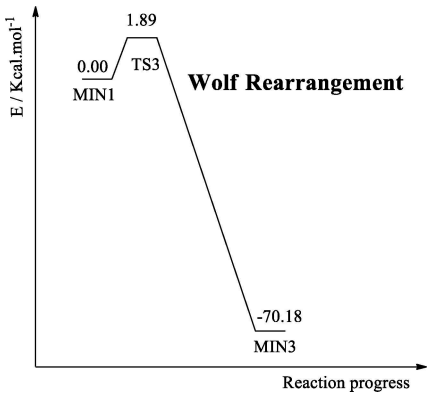

Figure 4. The one step reaction profile of Wolff Rearrangement.

Acknowledgements

The authors gratefully acknowledge the Payame Noor University Research Council for the financial support of this work.

Conflict of Interest

The authors declare no conflict of interest.

Keywords: bicyclo[2.1.0]pentanone · odd electron density · potential energy surface · unsaturated diazoketone · Wolff rearrangement

[1] G. Stork, J. Ficini, *J. Am. Chem. Soc.* **1961**, *83*, 4678.
[2] M. M. Fawzi, C. D. Gutsche, *J. Org. Chem.* **1966**, *31*, 1390.
[3] a) A. L. Wilds, J. van den Berghe, C. H. Winestock, R. L. von Trebra, N. F. Woolsey, *J. Am. Chem. Soc.* **1962**, *84*, 1503; b) A. L. Wilds, N. F. Woolsey, J. van den Berghe, C. H. Wine-stock, *Tetrahedron Lett.* **1965**, 4841; c) A. L. Wilds, R. L. von Trebra, N. F. Woolsey, *J. Org. Chem.* **1969**, *34*, 2401.
[4] S. Masamune, K. Fukumoto, *Tetrahedron Lett.* **1965**, *6*, 4647.
[5] a) C.-Y. Ho, F. T. Bond, *J. Am. Chem. Soc.* **1974**, *96*, 7355; b) F. T. Bond, C.-Y. Ho, *J. Org. Chem.* **1976**, *41*, 1421.
[6] W. Kirmse, *Eur. J. Org. Chem.* **2002**, 2002, 2193.
[7] a) B. Saha, G. Bhattacharjee, U. R. Ghatak, *Tetrahedron Lett.* **1986**, *27*, 3913; b) B. Saha, G. Bhattacharjee, U. R. Ghatak, *J. Chem. Soc. Perkin Trans. 1* **1988**, 939.
[8] a) P. Ceccherelli, M. Curini, M. C. Marcotullio, Rosati, O. Dirhodium, *Gazz. Chim. Ital.* **1994**, *124*, 177; b) P. Ceccherelli, M. Curini, F. Epifano, M. C. Marcotullio, O. Rosati, *Synth. Commun.* **1995**, *25*, 301.
[9] H. Seki, G. I. Georg, *J. Am. Chem. Soc.* **2010**, *132*, 15512.
[10] W. Sander, A. Strehl, A. R. Maguire, S. Collins, P. G. Kelleher, *Eur. J. Org. Chem.* **2000**, 3329.
[11] S. Fuse, Y. Otake, H. Nakamura, *Eur. J. Org. Chem.* **2017**, 6466.
[12] a) S. Motallebi, P. Müller, *Chimia* **1992**, *46*, 119; b) S. Motallebi, P. Müller, *Chim. Acta* **1993**, *76*, 2803; c) A. Safrygin, D. Dar′in, G. Kantin, M. Krasavin, *Eur. J. Org. Chem.* **2019**, 4721; d) K. Burger, J. Spengler, *Eur. J. Org. Chem.* **2000**, 199.
[13] a) A. B. Smith, III, *J. Chem. Soc. Chem. Commun.* **1974**, 695; b) A. B. Smith, III, B. H. Toder, S. J. Branca, R. K. Dieter, *J. Am. Chem. Soc.* **1981**, *103*, 1996; c) A. B. Smith, III, B. H. Toder, S. J. Branca, *J. Am. Chem. Soc.* **1984**, *106*, 3995; d) A. B. Smith, III, B. H. Toder, S. J. Branca, *J. Am. Chem. Soc.* **1984**, *106*, 4001.
[14] Gaussian 09, Revision **E.01**, M. J. Frisch, G. W. Trucks, H. B. Schlegel, G. E. Scuseria, M. A. Robb, J. R. Cheeseman, G. Scalmani, V. Barone, B. Mennucci, G. A. Petersson, H. Nakatsuji, M. Caricato, X. Li, H. P. Hratchian, A. F. Izmaylov, J. Bloino, G. Zheng, J. L. Sonnenberg, M. Hada, M. Ehara, K. Toyota, R. Fukuda, J. Hasegawa, M. Ishida, T. Nakajima, Y. Honda, O. Kitao, H. Nakai, T. Vreven, J. A. Montgomery, Jr., J. E. Peralta, F. Ogliaro, M. Bearpark, J. J. Heyd, E. Brothers, K. N. Kudin, V. N. Staroverov, R. Kobayashi, J. Normand, K. Raghavachari, A. Rendell, J. C. Burant, S. S. Iyengar, J. Tomasi, M. Cossi, N. Rega, J. M. Millam, M. Klene, J. E. Knox, J. B. Cross, V. Bakken, C. Adamo, J. Jaramillo, R. Gomperts, R. E. Stratmann, O. Yazyev, A. J. Austin, R. Cammi, C. Pomelli, J. W. Ochterski, R. L. Martin, K. Morokuma, V. G. Zakrzewski, G. A. Voth, P. Salvador, J. J. Dannenberg, S. Dapprich, A. D. Daniels, Ö. Farkas, J. B. Foresman, J. V. Ortiz, J. Cioslowski, and D. J. Fox, Gaussian, Inc., Wallingford CT, **2009**.
[15] Y. Zhao, D. G. Truhlar, *Theor. Chem. Acc.* **2006**, *120*, 215.
[16] T. Lu, F. Chen, *J. Comput. Chem.* **2012**, *33*, 580.
[17] A. M. Koster, P. Calaminici, M. E. Casida, R. Dominguez, V. D. Flores-Moreno, G. Geudtner, A. Goursot, T. Heine, A. Ipatov, F. Janetzko. J. M. del Campo, J. U. Reveles, A. Vela, B. Zuniga-Gutierrez, D. R. Salahub, deMon, Version 1, The deMon developers, Cinvestav, Mexico City, **2006**.

Manuscript received: February 26, 2021
Revised manuscript received: June 12, 2021